AIAA 2003-1450

Closed-Loop Deployable Structures

W.W. Gan and S. Pellegrino
University of Cambridge, Cambridge, CB2 1PZ, UK

44th AIAA/ASME/ASCE/AHS/ASC Structures, Structural Dynamics, and Materials Conference
7-10 April 2003
Norfolk, VA

Closed-Loop Deployable Structures

W.W. Gan* and S. Pellegrino†
University of Cambridge, Cambridge, CB2 1PZ, UK

This paper is concerned with a novel kind of deployable structures that form closed loops that fold into a bundle of bars using simple hinges. These structures, first envisaged by Dr J.M. Hedgepeth, have potential applications for ultra-lightweight solar arrays, solar sails, and radar structures. A systematic study of the kinematics of closed-loop structures is carried out, and a scheme for simulating the deployment of both symmetric and non-symmetric linkages is presented.

Introduction and Background

Many deployable structures form single or multiple, often interlaced, closed loops. Some of these structures form space frames, and have already had a variety of applications,[1,2] but this paper is concerned with a different type of structure, a kind of mechanical linkage that forms a segmented hoop that folds into a bundle of bars.

The first application of this type of structure was envisaged, to our knowledge, in a study co-authored by J.M. Hedgepeth in 1973.[3] Figure 1 shows an example of the main solution proposed, which was later adopted in the edge beam of the Hoop-Column Antenna, see Figure 2. In these structures the rim consists of an even number (four or more) of equal-length hinged segments and each joint involves two hinges and an intermediate block. However, Appendix A of Ref. [3] considered an alternative hinging method, which apparently had been suggested by A. Buseman during a progress review meeting at NASA Langley.[4]

This alternative solution is illustrated in Figure 3 and is the object of the present study. An advantage over the previous scheme is that it requires half the number of hinges and can provide better controlled deployment. Although new as a deployable structure, the four-sided version of this linkage is an example of the classical 4-bar linkage discovered in 1903 by the Cambridge mathematician G.T. Bennett.[5] The six-sided version of this linkage was also known, as it had been discovered by M. Goldberg in 1943.[6] It is shown as model H on the right-hand side of Figure 4, together with many other models made by Goldberg.

Structures of this kind have potential applications for solar arrays —as envisaged in Ref. [3]— and also solar sails. They could also be used to deploy and support flexible active surface for SAR structures. Here the configuration that is most frequently required is rectangular, and preliminary studies of closed-loop structures whose fully-deployed configuration is rectangular have been carried out.[7] For example, Figure 5 shows a six-bar structure with self-locking hinges that forms a rectangular frame.

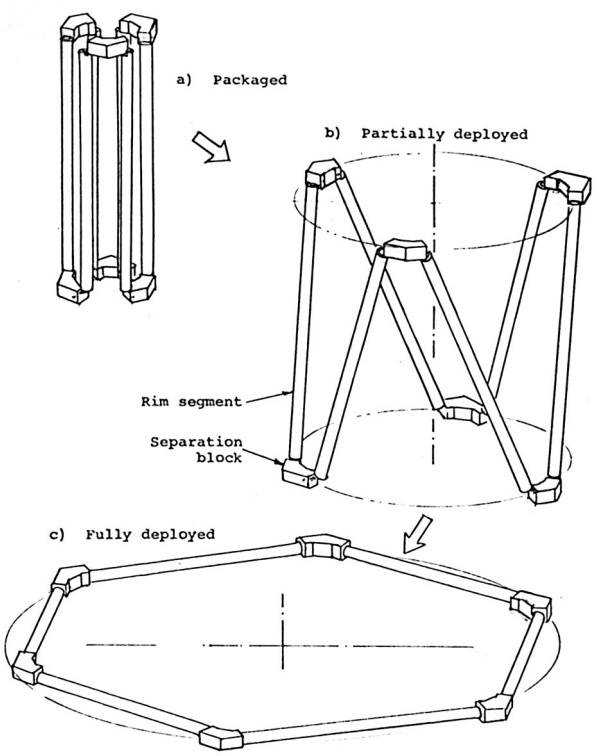

Fig. 1 Two-hinge method for deploying rim (from Ref. [3]).

In this paper we present a systematic study of the kinematics of closed-loop structures. The proposed approach is suitable for both symmetric linkages —such as those envisaged in Ref. [3]— and for much less symmetric structures such as that of Figure 5.

Modelling of Closed-Loop Linkages

A general formulation for linkages connected by revolute joints is naturally set up by considering a series of sets of cartesian coordinate axes, as explained next.

Given a fixed coordinate system, O, X, Y, Z, the general position and orientation of a local coordinate system, P_1, x_1, y_1, z_1, can be described by a translation

*Research Student, Department of Engineering, Trumpington Street.

†Professor of Structural Engineering, Department of Engineering, Trumpington Street. Associate Fellow AIAA. pellegrino@eng.cam.ac.uk

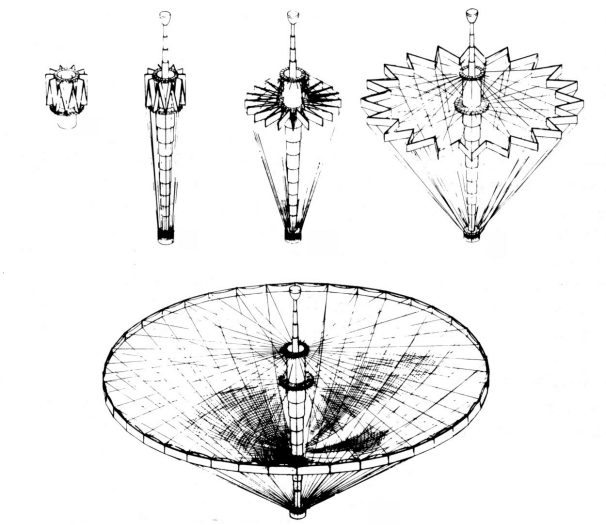

Fig. 2 Deployment of Hoop-Column Antenna (from Ref. [3]).

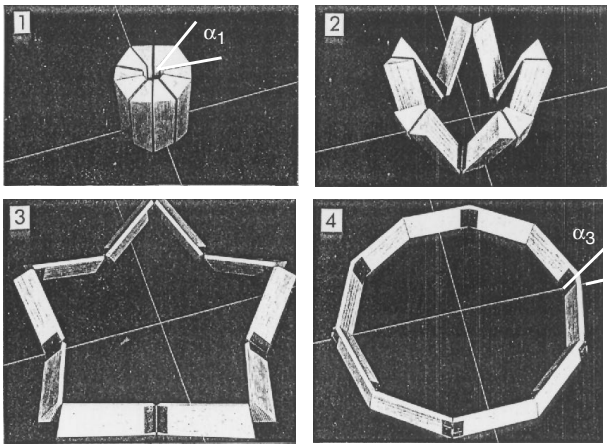

Fig. 3 One-hinge method for deploying rim (from Ref. [3]).

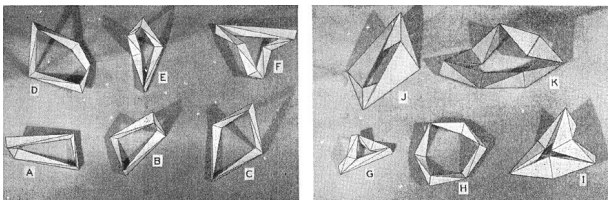

Fig. 4 Models made by Goldberg (from Ref. [6]).

Fig. 5 Deployable 6-bar structure with self-locking hinges.

from O to P_1 followed by a rotation to P_1, x_1, y_1, z_1. The two quantities that describe this transformation are a vector v_1 (3×1) and a matrix R_1 (3×3). Following Denavit and Hartenberg[8] it is convenient to write them as a single 4×4 matrix

$$T_1 = \begin{bmatrix} & R_1 & & v_1 \\ 0 & 0 & 0 & 1 \end{bmatrix} \tag{1}$$

Here R_1 is defined according to the standard x-convention for the Euler angles ϕ, ω, ψ that transform the global coordinates system into x_1, y_1, z_1[9]

$$R_1 = \begin{bmatrix} \cos\phi & -\sin\phi & 0 \\ \sin\phi & \cos\phi & 0 \\ 0 & 0 & 1 \end{bmatrix} \begin{bmatrix} 1 & 0 & 0 \\ 0 & \cos\omega & -\sin\omega \\ 0 & \sin\omega & \cos\omega \end{bmatrix} \begin{bmatrix} \cos\psi & -\sin\psi & 0 \\ \sin\psi & \cos\psi & 0 \\ 0 & 0 & 1 \end{bmatrix} \tag{2}$$

Note that R_1 transforms the local coordinates x_1, y_1, z_1 into the global coordinates X,Y,Z.

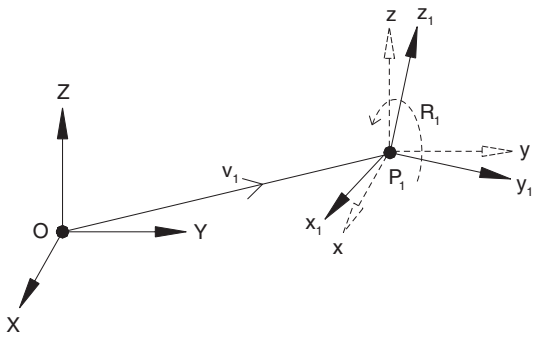

Fig. 6 General transformation of a coordinate system.

Next, consider a further transformation of this set of axes, from P_1, x_1, y_1, z_1 to P_2, x_2, y_2, z_2 as shown in Figure 7. This transformation is represented by

$$T_2 = \begin{bmatrix} & R_2 & & v_2 \\ 0 & 0 & 0 & 1 \end{bmatrix} \tag{3}$$

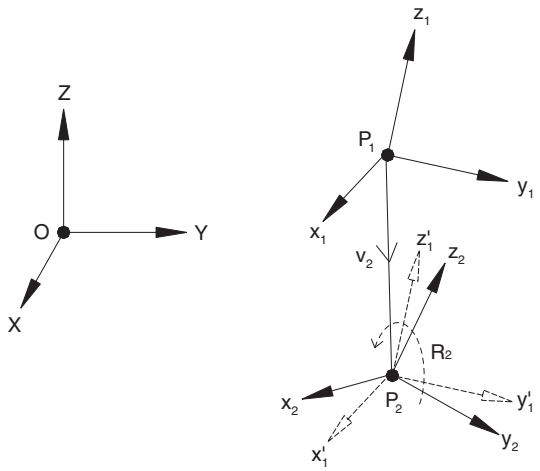

Fig. 7 Transformation from P_1, x_1, y_1, z_1 to P_2, x_2, y_2, z_2.

where $v_2 = P_1P_2$ and its components are defined in the local coordinate system P_1, x_1, y_1, z_1 and hence transform from P_1, x_1, y_1, z_1 to P_2, x_2, y_2, z_2. The relative rotation R_2 transforms from the system x_2, y_2, z_2 to x_1, y_1, z_1; note that this goes in the opposite direction to v_2.

Consider the compound transformation $T_{1,2}$, i.e. T_1 followed by T_2. The translation vector is v_1 followed by R_1v_2, because the second translation needs to be transformed to the first coordinate system, hence

$$v_{1,2} = v_1 + R_1v_2 \tag{4}$$

The rotation matrix is obtained from

$$\begin{aligned} X &= R_1x_1 \\ x_1 &= R_2x_2 \end{aligned}$$

Hence,

$$X = R_1R_2x_2 \tag{5}$$

Therefore, clearly

$$T_{1,2} = \begin{bmatrix} & R_1R_2 & & v_1 + R_1v_2 \\ 0 & 0 & 0 & 1 \end{bmatrix} \tag{6}$$

This can also be obtained by post-multiplying T_1 by T_2:

$$\begin{aligned} T_1 \times T_2 &= \begin{bmatrix} & R_1 & & v_1 \\ 0 & 0 & 0 & 1 \end{bmatrix} \begin{bmatrix} & R_2 & & v_2 \\ 0 & 0 & 0 & 1 \end{bmatrix} \\ &= \begin{bmatrix} & R_1R_2 & & v_1 + R_1v_2 \\ 0 & 0 & 0 & 1 \end{bmatrix} \end{aligned} \tag{7}$$

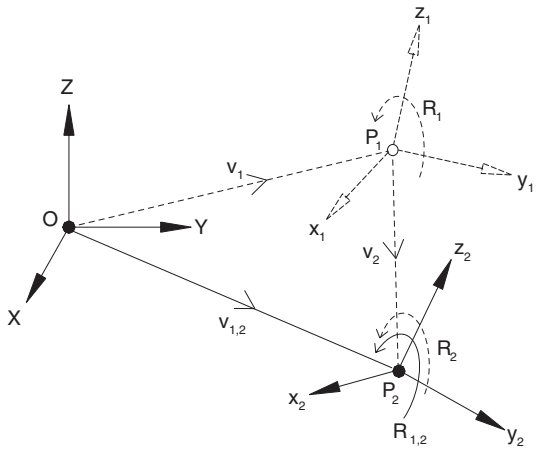

Fig. 8 Compound transformation $T_{1,2}$, i.e. T_1 followed by T_2.

A more general compound transformation, consisting of n transformations can be expressed as

$$\begin{aligned} T_{1,n} &= T_1 \times T_2 \times \ldots \times T_n \\ &= \begin{bmatrix} & R_1 & & v_1 \\ 0 & 0 & 0 & 1 \end{bmatrix} \ldots \begin{bmatrix} & R_n & & v_n \\ 0 & 0 & 0 & 1 \end{bmatrix} \end{aligned} \tag{8}$$

and is useful in describing the configurations of a linkage of n rods connected by revolute joints.

Closed Loop Linkages

We will describe a general method of analysis for closed loop linkages consisting of n rods connected by revolute joints. We will describe first the case $n = 4$, which corresponds to a Bennett linkage. Figure 9 shows a square framework that folds into a compact bundle of rods. This model is made from wooden bars connected together by "door" hinges. During folding, the model preserves two planes of symmetry, and one 2-fold symmetry axis.

Single Rod with 2 Joints

Consider a rod with two non-parallel revolute joints attached to the ends. Its geometry can be represented by the transformation matrix T_1, where v describes the direction and length of the member and R describes the relative orientation of the two joints. If the rod has unit length ($a^2+d^2 = 1$), we have

$$v = \begin{bmatrix} a \\ 0 \\ d \end{bmatrix} = \begin{bmatrix} \frac{\sqrt{6}}{3} \\ 0 \\ \frac{\sqrt{3}}{3} \end{bmatrix}$$

The relative orientation of the two revolute joints is obtained by performing a series of elementary rotations ϕ, ω and ψ, respectively, about the z, ξ' and ζ'

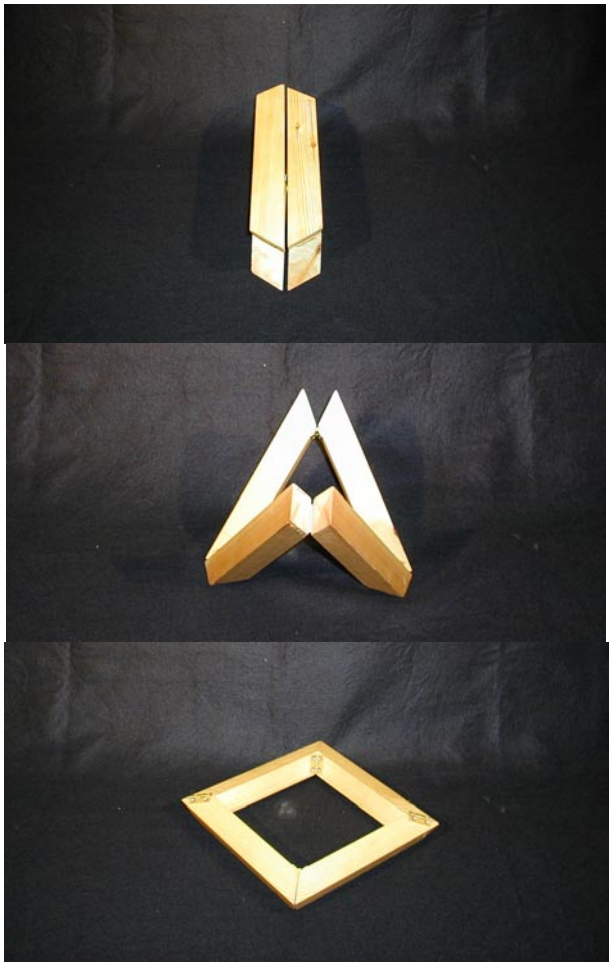

Fig. 9 Model of four-member frame (Bennett linkage).

axes, as shown in Figure 10. Here

$$\begin{aligned} \phi &= -30^\circ \\ \omega &= +90^\circ + \tan^{-1}(1/\sqrt{8}) = +109.47^\circ \\ \psi &= -150^\circ \end{aligned}$$

The corresponding transformation matrix is

$$T_1 = \begin{bmatrix} -\frac{2}{3} & \frac{\sqrt{3}}{3} & -\frac{\sqrt{2}}{3} & \frac{\sqrt{6}}{3} \\ \frac{\sqrt{3}}{3} & 0 & -\frac{\sqrt{6}}{3} & 0 \\ -\frac{\sqrt{2}}{3} & -\frac{\sqrt{6}}{3} & -\frac{1}{3} & \frac{\sqrt{3}}{3} \\ 0 & 0 & 0 & 1 \end{bmatrix}$$

Two Rods Connected by a Joint

Consider the two rods OP_1 and P_2P_3, as shown in Figure 11, connected at point A where $P_1 = P_2$. The second member P_2P_3 is arranged in such a way that x_1 is collinear with x_2 when the hinge rotation θ_A is zero.

We can write the following expression for the trans-

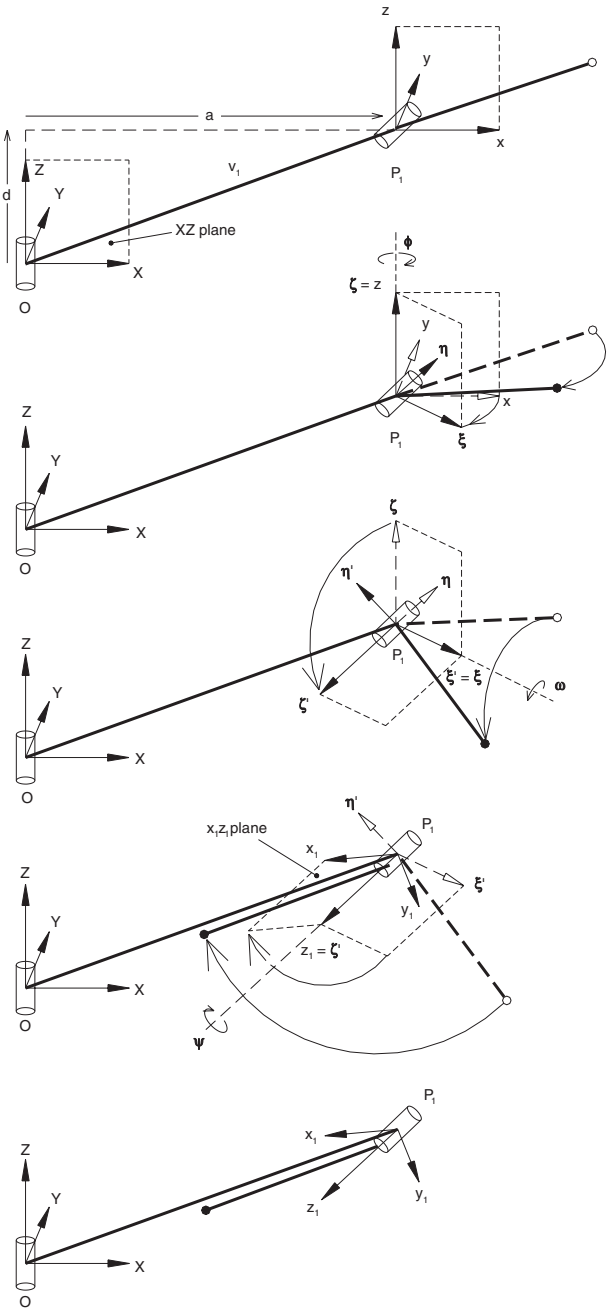

Fig. 10 Formulation of transformation matrix for element of Bennett linkage.

formation matrix

$$\begin{aligned} T_{1,3} &= T_1 \times T_{\theta_A} \times T_3 \\ &= \begin{bmatrix} & R_1 & & v_1 \\ 0 & 0 & 0 & 1 \end{bmatrix} \begin{bmatrix} \cos\theta_A & -\sin\theta_A & 0 & 0 \\ \sin\theta_A & \cos\theta_A & 0 & 0 \\ 0 & 0 & 1 & 0 \\ 0 & 0 & 0 & 1 \end{bmatrix} \\ &\quad \begin{bmatrix} & R_3 & & v_3 \\ 0 & 0 & 0 & 1 \end{bmatrix} \end{aligned}$$

Note that the hinge rotation appears only in the ma-

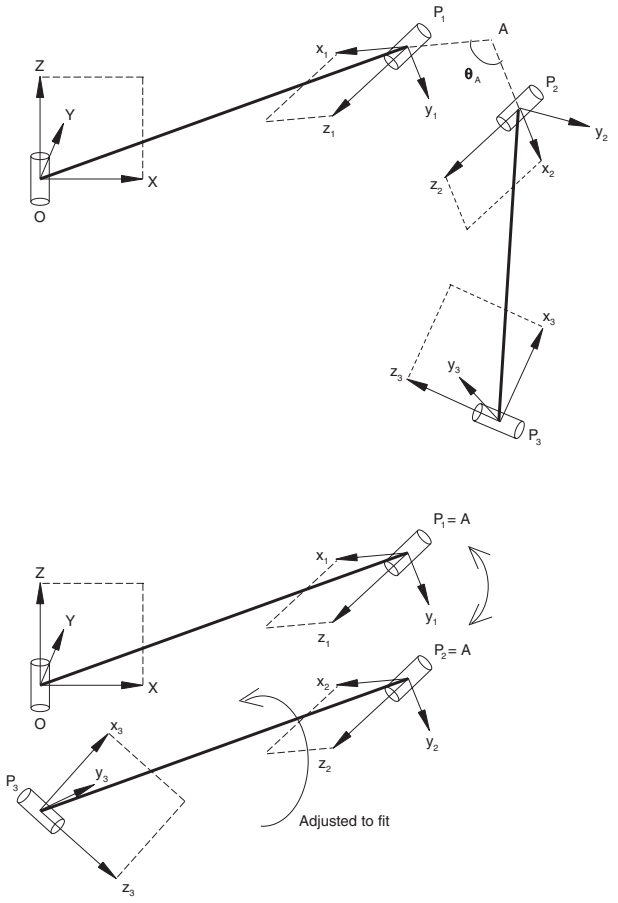

Fig. 11 Two rods of a Bennett linkage.

trix in the middle; T_1 and T_3 are constant.

Closed Loop of Four Rods

By an obvious extension of the above two-rod example we can formulate a closed-loop, four-rod linkage as the product of four constant matrices and four angle-dependent matrices:

$$T_1 \times T_{\theta_A} \times T_3 \times T_{\theta_B} \times T_1 \times T_{\theta_C} \times T_3 \times T_{\theta_D} = I \quad (9)$$

Here, the identity matrix on the right-hand-side imposes the condition that the loop should remain closed in all configurations, and hence (i) the first and last points are the same, and (ii) the axes of rotation of the first and last revolute joints coincide. We will call this equation the *loop closure equation*.

Loop of n Rods

Consider a closed loop of the type shown in Figure 3, consisting of n rods with identical cross-section, their cross-section being isosceles triangles. For these rods to fit together as a bundle in the folded configuration, the apex angle of the isosceles triangle must be

$$\alpha_1 = \frac{2\pi}{n} \quad (10)$$

We also define

$$\alpha_2 = \frac{1}{2}\alpha_1 \quad (11)$$

Finally, consider a radial section of the structure in its deployed configuration, Figure 3, through one of the hinges. This section is also an isosceles triangle, and the angles at the base are

$$\alpha_3 = \arctan(\sin\alpha_2 \tan\alpha_2) \quad (12)$$

The hinges are mounted alternately on the inner and outer side faces of the isosceles triangles.

Hence, we can obtain the following expressions for the angles ϕ, ω, ψ and the lengths a, d

$$\begin{aligned} \phi_1 &= -\arctan(\tan\alpha_2 \sin\alpha_3) \\ \omega_1 &= \frac{\pi}{2} + \arctan\frac{y}{\sqrt{x^2+z^2}} \\ \psi_1 &= -\pi - \phi_1 \\ a_1 &= \cos\alpha_3 \\ d_1 &= \sin\alpha_3 \end{aligned}$$

where

$$\begin{aligned} x &= \cos\alpha_3 \tan\alpha_3 - \sin\alpha_3 \cos\alpha_1 \\ y &= \sin\alpha_3 \tan\alpha_3 + \cos\alpha_3 \cos\alpha_1 \\ z &= \sin\alpha_1 \end{aligned}$$

The corresponding expressions for the second rod are

$$\begin{aligned} \phi_2 &= -\phi_1 \\ \omega_2 &= -\omega_1 \\ \psi_2 &= -\psi_1 \\ a_2 &= a_1 \\ d_2 &= d_1 \end{aligned}$$

Using these expressions, we can set up the loop closure equation for this linkage. It is analogous to Equation 9, but now includes n constant matrices and n angle-dependent matrices.

The hinge angle for which the linkage is fully deployed is

$$\theta_A = \arccos[1 - 2\cos^2\alpha_3(\sin(\frac{\pi}{2} - \frac{\pi}{N}) + \sin^2\alpha_2 \tan\alpha_3)^2]$$

Analytical Solution of Loop Closure Equation

For the Bennett linkage symmetry can be assumed, hence $\theta_A = \theta_C$ and $\theta_B = \theta_D$. Thus, Equation 9 can be simplified to

$$\left\{ \begin{bmatrix} -\frac{2}{3} & \frac{\sqrt{3}}{3} & -\frac{\sqrt{2}}{3} & \frac{\sqrt{6}}{3} \\ \frac{\sqrt{3}}{3} & 0 & -\frac{\sqrt{6}}{3} & 0 \\ -\frac{\sqrt{2}}{3} & -\frac{\sqrt{6}}{3} & -\frac{1}{3} & \frac{\sqrt{3}}{3} \\ 0 & 0 & 0 & 1 \end{bmatrix} \begin{bmatrix} \cos\theta_2 & -\sin\theta_A & 0 & 0 \\ \sin\theta_A & \cos\theta_A & 0 & 0 \\ 0 & 0 & 1 & 0 \\ 0 & 0 & 0 & 1 \end{bmatrix} \right.$$
$$\left. \begin{bmatrix} -\frac{2}{3} & -\frac{\sqrt{3}}{3} & -\frac{\sqrt{2}}{3} & \frac{\sqrt{6}}{3} \\ -\frac{\sqrt{3}}{3} & 0 & \frac{\sqrt{6}}{3} & 0 \\ -\frac{\sqrt{2}}{3} & \frac{\sqrt{6}}{3} & -\frac{1}{3} & \frac{\sqrt{3}}{3} \\ 0 & 0 & 0 & 1 \end{bmatrix} \begin{bmatrix} \cos\theta_B & -\sin\theta_B & 0 & 0 \\ \sin\theta_B & \cos\theta_B & 0 & 0 \\ 0 & 0 & 1 & 0 \\ 0 & 0 & 0 & 1 \end{bmatrix} \right\}^2 = I$$

and solving this equation symbolically yields

$$\begin{aligned}\theta_B &= \tan^{-1}\Big(2\sqrt{3}\cos^2\theta_A - 3\sin\theta_A\cos\theta_A \\ &\quad +3\sin\theta_A - 4\sqrt{3}\cos\theta_A + 2\sqrt{3}\Big) \\ &\quad \Big/\Big(-\cos^2\theta_A - 2\sqrt{3}\sin\theta_A\cos\theta_A \\ &\quad +2\sqrt{3}\sin\theta_A - \cos\theta_A + 2\Big) \qquad (13)\end{aligned}$$

A plot of θ_A against θ_B is shown in Figure 12.

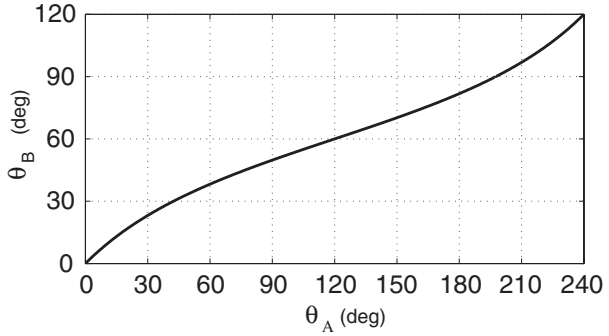

Fig. 12 θ_A vs θ_B for Bennett linkage.

Numerical Solution of Closure Equation

Here we present a general solution method, based on a predictor-corrector scheme suitable for implementation in a standard Newton-Raphson iteration, for the loop closure equation. For definiteness, we refer to a Bennett linkage. We assume that the linkage is given in its initial configuration, e.g. the hinge angle s θ_{A_0}, θ_{B_0}, θ_{C_0} and θ_{D_0} are equal to zero and all four rods fit together as a bundle.

Predictor Step

From the closure equation

$$T_1\ T_{A_0}\ T_3\ T_{B_0}\ T_1\ T_{C_0}\ T_3\ T_{D_0} = I \qquad (14)$$

Consider small geometry changes in each hinge with zero strain or deformation in the rods. For the linkage to remain intact it needs to satisfy the equation:

$$T_1\ T_A\ T_3\ T_B\ T_1\ T_C\ T_3\ T_D = I \qquad (15)$$

where T_A, T_B, T_C and T_D correspond to the general configuration defined by θ_A, θ_B, θ_C and θ_D. Consider the Taylor expansion of the hinge angles. By ignoring higher-order terms we have

$$\begin{aligned}\sin(\theta_{A_0}+\Delta\theta_{A_0}) &\approx \sin\theta_{A_0} + \cos\theta_{A_0}(\Delta\theta_{A_0}) \\ \cos(\theta_{A_0}+\Delta\theta_{A_0}) &\approx \cos\theta_{A_0} - \sin\theta_{A_0}(\Delta\theta_{A_0})\end{aligned}$$

Substituting into, e.g. the transformation matrix T_A, yields

$$\begin{aligned}T_A &= \begin{bmatrix}\cos(\theta_{A_0}+\Delta\theta_{A_0}) & -\sin(\theta_{A_0}+\Delta\theta_{A_0}) & 0 & 0\\ \sin(\theta_{A_0}+\Delta\theta_{A_0}) & \cos(\theta_{A_0}+\Delta\theta_{A_0}) & 0 & 0\\ 0 & 0 & 1 & 0\\ 0 & 0 & 0 & 1\end{bmatrix} \\ &\simeq T_{A_0} + \begin{bmatrix}-\sin\theta_{A_0} & -\cos\theta_{A_0} & 0 & 0\\ \cos\theta_{A_0} & -\sin\theta_{A_0} & 0 & 0\\ 0 & 0 & 0 & 0\\ 0 & 0 & 0 & 0\end{bmatrix}\Delta\theta_{A_0} \\ &= T_{A_0} + U_{A_0}\,\Delta\theta_{A_0} \qquad (16)\end{aligned}$$

where U_{A_0} is the derivative of T_A calculated at A_0.

Substituting Equation 16 and similar into (14) yields

$$T_1\,(T_{A_0}+U_{A_0}\Delta\theta_{A_0})\ T_3\,(T_{B_0}+U_{B_0}\Delta\theta_{B_0})\cdots = I \quad (17)$$

Expanding Equation 17 and rearranging, we have

$$\begin{aligned}&T_1T_{A_0}T_3T_{B_0}T_1T_{C_0}T_3T_{F_0} \\ &+(T_1U_{A_0}T_3T_{B_0}T_1T_{C_0}T_3T_{D_0})\,\Delta\theta_{A_0} \\ &+(T_1T_{A_0}T_3U_{B_0}T_1T_{C_0}T_3T_{D_0})\,\Delta\theta_{B_0} \\ &+(T_1T_{A_0}T_3T_{B_0}T_1U_{C_0}T_3T_{D_0})\,\Delta\theta_{C_0} \\ &+(T_1T_{A_0}T_3T_{B_0}T_1T_{C_0}T_3U_{D_0})\,\Delta\theta_{D_0} \quad = I \quad (18)\end{aligned}$$

From Equation 14, the first term of Equation 18 is equal to the identity matrix. Hence, the sum of the remaining terms must be zero. Defining $A = T_1U_{A_0}T_3T_{B_0}T_1T_{C_0}T_3T_{D_0}$, etc. this equation can be rearranged into

$$A\,\Delta\theta_{A_0} + B\,\Delta\theta_{B_0} + C\,\Delta\theta_{C_0} + D\,\Delta\theta_{D_0} = [0] \quad (19)$$

where $[0]$ is a 4×4 null matrix. It is interesting to note the form of these matrices

$$\begin{aligned}&\begin{bmatrix}0 & a_{1,2} & a_{1,3} & a_{1,4}\\ -a_{1,2} & 0 & a_{2,3} & a_{2,4}\\ -a_{1,3} & -a_{2,3} & 0 & a_{3,4}\\ 0 & 0 & 0 & 0\end{bmatrix}\Delta\theta_{A_0} \\ &+\begin{bmatrix}0 & b_{1,2} & b_{1,3} & b_{1,4}\\ -b_{1,2} & 0 & b_{2,3} & b_{2,4}\\ -b_{1,3} & -b_{2,3} & 0 & b_{3,4}\\ 0 & 0 & 0 & 0\end{bmatrix}\Delta\theta_{B_0} + \ldots \quad = [0] \quad (20)\end{aligned}$$

At first glance, the matrix equation (20) would appear to be equivalent to 9 scalar equations in 4 unknowns, not 16, since the 7 equations corresponding to the diagonal and the last row are always satisfied. The fact that the 3×3 sub-matrix in the top-left corner is skew-symmetric corresponds to the fact that any rotation can always be defined by only three elementary rotations, hence 6 of the 9 coefficients of this sub-matrix are dependent on the other 3.

Hence, this yields a 6×4 system of equations

$$\begin{bmatrix} a_{1,2} & b_{1,2} & c_{1,2} & d_{1,2} \\ a_{1,3} & b_{1,3} & c_{1,3} & d_{1,3} \\ a_{2,3} & b_{2,3} & c_{2,3} & d_{2,3} \\ a_{1,4} & b_{1,4} & c_{1,4} & d_{1,4} \\ a_{2,4} & b_{2,4} & c_{2,4} & d_{2,4} \\ a_{3,4} & b_{3,4} & c_{3,4} & d_{3,4} \end{bmatrix} \begin{bmatrix} \Delta\theta_{A_0} \\ \Delta\theta_{B_0} \\ \Delta\theta_{C_0} \\ \Delta\theta_{D_0} \end{bmatrix} = \begin{bmatrix} 0 \\ 0 \\ 0 \\ 0 \\ 0 \\ 0 \end{bmatrix} \tag{21}$$

The rank of the matrix in Equation 21 equals 3, which implies that the equation has a single infinity of solutions. This also indicates that the linkage has an internal mechanism. By solving Equation 21 we can find sets of $\Delta\theta\ 's \neq 0$ which describe infinitesimal, zero-strain motions of the linkage.

Corrector Step

A finite, yet small motion of the linkage where each hinge angle is changed by an amount proportional to the infinitesimal mechanism computed above is likely to induce small errors.

Let $\bar{C}$ be a configuration obtained from the predictor step, i.e. by imposing a small, and yet finite change of angles to the initial configuration. We wish to compute a configuration C_1, near $\bar{C}$, where all errors have been removed. Hence, we need to compute $\Delta C'$, the configuration change from $\bar{C}$ to C_1.

In configuration C_1 we will have

$$T_1\ T_{A_1}\ T_3\ T_{B_1}\ T_1\ T_{C_1}\ T_3\ T_{D_1} = I \tag{22}$$

Although we do not know C_1, we do know $\bar{C}$. In this configuration the closure equation is not satisfied, hence we can compute an error matrix E from

$$T_1\ T_{\bar{A}}\ T_3\ T_{\bar{B}}\ T_1\ T_{\bar{C}}\ T_3\ T_{\bar{D}} = I + E \tag{23}$$

Expanding the hinge angles in configuration C_1 in term of $\bar{C}$, we have

$$\theta_{A_1} = \theta_{\bar{A}} + \Delta\theta'_A, \quad \theta_{B_1} = \theta_{\bar{B}} + \Delta\theta'_B, \quad \ldots$$

Now, writing the closure equation in configuration C_1, substituting a Taylor expansion for each hinge angle, and then manipulating the equations as above we obtain

$$\begin{aligned} & T_1 T_{\bar{A}} T_3 T_{\bar{B}} T_1 T_{\bar{C}} T_3 T_{\bar{D}} \\ & +(T_1 U_{\bar{A}} T_3 T_{\bar{B}} T_1 T_{\bar{C}} T_3 T_{\bar{D}})\ \Delta\theta'_A \\ & +(T_1 T_{\bar{A}} T_3 U_{\bar{B}} T_1 T_{\bar{C}} T_3 T_{\bar{D}})\ \Delta\theta'_B \\ & +(T_1 T_{\bar{A}} T_3 T_{\bar{B}} T_1 U_{\bar{C}} T_3 T_{\bar{D}})\ \Delta\theta'_C \\ & +(T_1 T_{\bar{A}} T_3 T_{\bar{B}} T_1 T_{\bar{C}} T_3 U_{\bar{D}})\ \Delta\theta'_D \quad = I \end{aligned} \tag{24}$$

From Equation 23, the first term in Equation 24 is equal to $I + E$. Hence substituting Equation 23 into Equation 24, we obtain

$$\begin{aligned} & +(T_1 U_{\bar{A}} T_3 T_{\bar{B}} T_1 T_{\bar{C}} T_3 T_{\bar{D}})\ \Delta\theta'_A \\ & +(T_1 T_{\bar{A}} T_3 U_{\bar{B}} T_1 T_{\bar{C}} T_3 T_{\bar{D}})\ \Delta\theta'_B \\ & +(T_1 T_{\bar{A}} T_3 T_{\bar{B}} T_1 U_{\bar{C}} T_3 T_{\bar{D}})\ \Delta\theta'_C \\ & +(T_1 T_{\bar{A}} T_3 T_{\bar{B}} T_1 T_{\bar{C}} T_3 U_{\bar{D}})\ \Delta\theta'_D = -E \end{aligned} \tag{25}$$

which can be written in form

$$P\,\Delta\theta'_A + Q\,\Delta\theta'_B + R\,\Delta\theta'_C + S\,\Delta\theta'_D = -E \tag{26}$$

where $P = T_1 U_{\bar{A}} T_3 T_{\bar{B}} T_1 T_{\bar{C}} T_3 T_{\bar{D}}$, $\ldots$ etc. The error matrix E on the right hand side has the structure

$$\begin{bmatrix} & & & e_{1,4} \\ & F & & e_{2,4} \\ & & & e_{3,4} \\ 0 & 0 & 0 & 0 \end{bmatrix}$$

We decompose F into its symmetric and skew-symmetric components, i.e. $(F + F^T)/2$, $(F - F^T)/2$, and consider only the skew-symmetric part, whose coefficients are denoted by $\bar{e}_{1,2}$, $\bar{e}_{1,3}$ and $\bar{e}_{2,3}$. This transformed equation can be treated in the same way as Equation 21, thus rearranging it into 6 scalar equations

$$\begin{bmatrix} p_{1,2} & q_{1,2} & r_{1,2} & s_{1,2} \\ p_{1,3} & q_{1,3} & r_{1,3} & s_{1,3} \\ p_{2,3} & q_{2,3} & r_{2,3} & s_{2,3} \\ p_{1,4} & q_{1,4} & r_{1,4} & s_{1,4} \\ p_{2,4} & q_{2,4} & r_{2,4} & s_{2,4} \\ p_{3,4} & q_{3,4} & r_{3,4} & s_{3,4} \end{bmatrix} \begin{bmatrix} \Delta\theta'_A \\ \Delta\theta'_B \\ \Delta\theta'_C \\ \Delta\theta'_D \end{bmatrix} = - \begin{bmatrix} \bar{e}_{1,2} \\ \bar{e}_{1,3} \\ \bar{e}_{2,3} \\ e_{1,4} \\ e_{2,4} \\ e_{3,4} \end{bmatrix} \tag{27}$$

The least squares solution of Equation 27 is used to determine the minimal correcting angles $\Delta\theta'$ due to the errors in configuration $\bar{C}$

$$\Delta\theta' = -\sum_{i=1}^{r} \frac{w_i\ u_i^T}{v_{i,i}}\, e \tag{28}$$

where $F = UVW^T$ is the singular value decomposition of the 6×4 coefficient matrix in Equation 27 and r is the number of non-zero singular values. Also, w_i is the i^{th} column of matrix W; u_i is the i^{th} column of U; $v_{i,i}$ is the i, i term in matrix V; $-e$ is the vector on the right hand side of Equation 27.

The predictor-corrector stages of the algorithm presented above are repeated until the hinges hit their physical stops, at which point the linkage is fully deployed.

Results

Using the above numerical solution method for the closure equation, we have analysed the deployment behaviour of the 4-rod linkage (Bennett linkage) but this time without assuming symmetric behaviour. Figure 13 shows a plot of the hinge angles variation during deployment; note that $\theta_B = \theta_D$ at all stages, hence confirming that the structure remains symmetric at all stages. Also note that the behaviour predicted by the numerical scheme is identical to the analytical results shown in Figure 12. Figure 14 shows six snapshots from the deployment sequence.

The same solution method, applied to the 6-rod linkage also predicts that the structure remains symmetric at all stages, see Figure 15 and Figure 16.

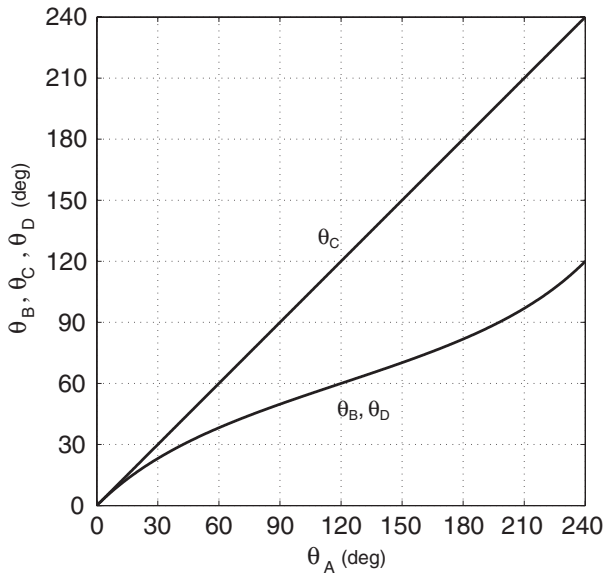

Fig. 13 Variation of hinge angles during deployment of 4-rod linkage.

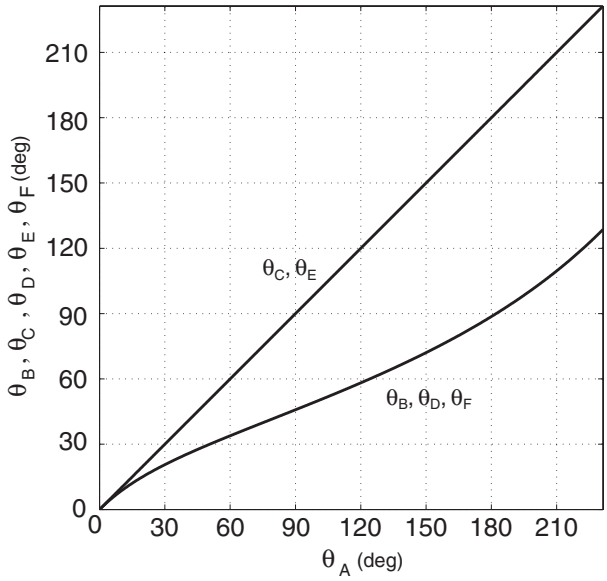

Fig. 15 Variation of hinge angles during deployment of 6-rod linkage.

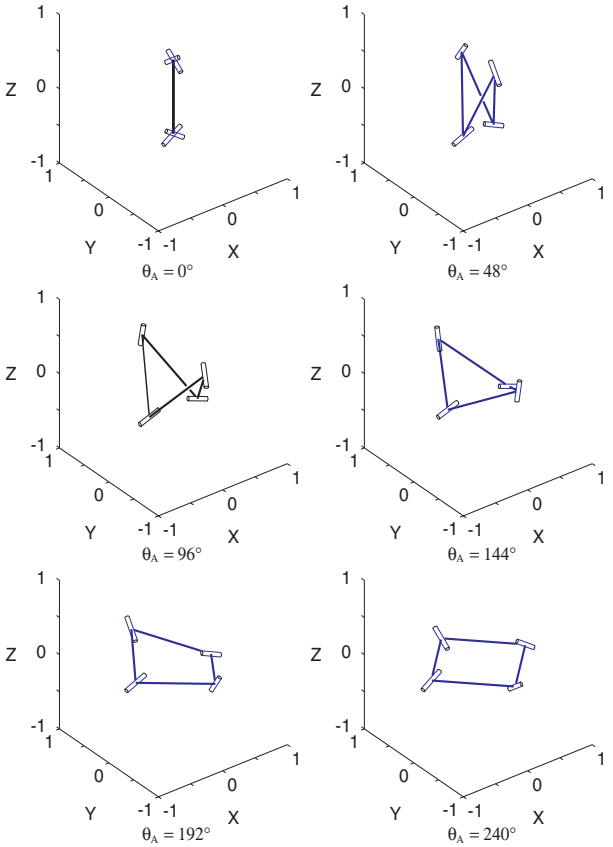

Fig. 14 Deployment sequence of 4-rod linkage.

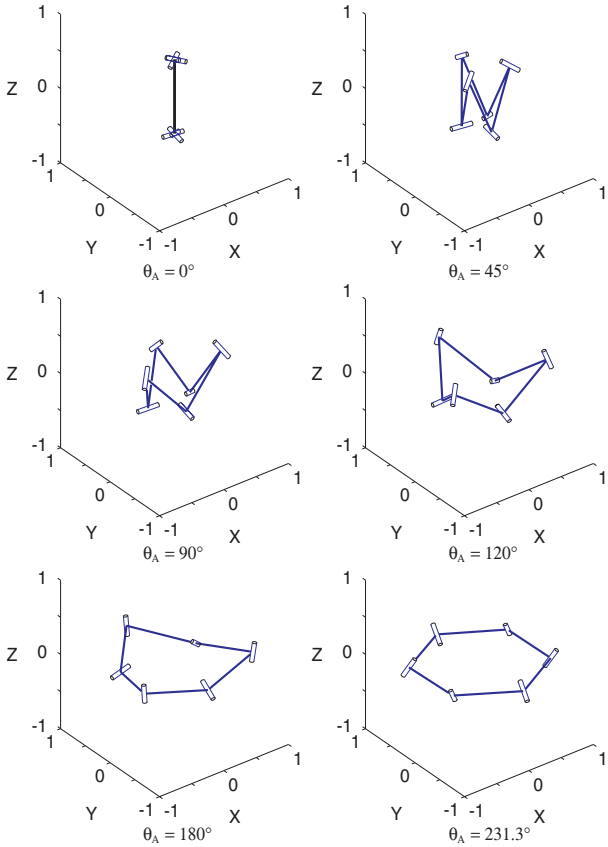

Fig. 16 Deployment sequence of 6-rod linkage.

Discussion

The formulation presented in this paper provides considerable insight into the kinematic behaviour of closed-loop linkages, from which issues important for design, such as sensitivity to imperfections, can be analysed. It also becomes possible to design assemblies with special properties, e.g. frames with some particular dimensions.

References

[1] Hoberman, C. (1991). Reversibly expandable structures. USA Patent No. 4981732.

[2] Pellegrino, S. and You, Z. (1993). Foldable ring structures. In Space Structures 4. Proceedings of Fourth International Conference on Space Structures, Guildford, 6-10 September 1993, (Edited by G.A.R. Parke and C.M. Howard), pp 783-792. Thomas Telford, London.

[3] Crawford, R. F., Hedgepeth, J. M. and Preiswerk, P. R. (1973). Spoked wheels to deploy large surfaces in space: weight estimates for solar arrays. NASA-CR-2347.

[4] Mikulas, M. (1998) Personal Communication.

[5] Bennett, G.T. (1903) A new mechanism, *Engineering* 76, 777-778.

[6] Goldberg, M. (1943). New Five-Bar and Six-Bar Linkages in Three Dimensions. Transactions of the ASME, 649-661.

[7] Pellegrino, S., Green, C., Guest, S.D. and Watt, A. (2000) SAR advanced deployable structure, Technical Report CUED/D-STRUCT/TR191, Department of Engineering, University of Cambridge.

[8] Denavit, J. and Hartenberg, R.S. (1955) A kinematic notation for lower-pair mechanisms based on matrices, Journal of Applied Mechanics, June 1955, 215-221.

[9] Goldstein, H. (1980). Classical Mechanics, Second Edition. Addison-Wesley, Reading, MA.